

OPTICAL MEASUREMENTS THROUGH PANORAMIC IMAGING SYSTEMS

by

John A. Gilbert, Donald R. Matthys, Pal Greguss¹

Abstract

Optical inspections and measurements are made on the inner surfaces of cavities using a unique panoramic annular lens (PAL) and a technique called radial metrology. The lens is described in detail, and examples of inspections and measurements made through PAL systems using laser scanning techniques, speckle photography, and holographic interferometry are included. Computer algorithms for detecting anomalies, digitally correlating images, and linearizing the annular images obtained from the PAL are also described.

Introduction

Optical methods have been used for decades to inspect and to make stress analysis measurements but most techniques have been applied on the outer surfaces of structural components. More recently, primarily due to the introduction of new tools such as fiber optics and microelectronic devices, it has become feasible to make measurements on interior and remote surfaces. However, fiber-based systems, as well as the more conventional non-fiber-based systems, suffer from a limited field of view. Ideally, an optical device for making measurements on the inner surface of a cavity should provide a panoramic view of the entire cavity.

The first attempt to design a system for panoramic imaging was made by Mangin in 1878.¹ Since that time, numerous devices have been patented.² These endeavors can be divided into two main groups: those in which the imaging device or a part of it is rotated around its axis to scan the area of interest, and those which utilize combinations of optical elements to obtain a single panoramic view. These optical elements may have several refracting/reflecting parts with collinear optical axes or may consist of a single block having several refracting and reflecting surfaces. Unfortunately, these compound systems are often difficult to manufacture and miniaturize if high quality panoramic images are needed. Scanning techniques^{3,4} also have disadvantages; beside the need for a rotating mechanism, no

simultaneous viewing of the entire space is possible. These constraints severely limit functional and real-time capabilities. Fortunately, many of the drawbacks of both compound and scanning systems were eliminated in the development of the panoramic annular lens.⁵

The Panoramic Annular Lens

The panoramic annular lens (PAL) consists of a single piece of glass with spherical surfaces that produces a flat annular image of the entire 360 degree surround of the optical axis of the lens. Figure 1, for example, is a photograph taken of Rockefeller Center with the PAL pointed toward the sky and shows the

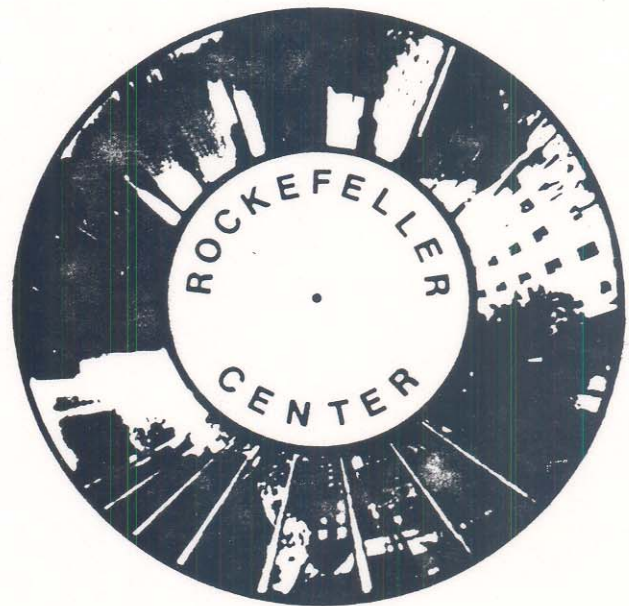


Figure 1. A photograph of Rockefeller Center taken by pointing a PAL camera toward the sky.

¹ J. Gilbert is Professor and Director of Civil Engineering, University of Alabama in Huntsville, Huntsville, Alabama; D. Matthys is Professor of Physics at Marquette University, Milwaukee, Wisconsin; and P. Greguss is Professor Emeritus at the Technical University of Budapest, Budapest, Hungary.

type of imaging that occurs. The mapping performed by the PAL to produce the annular image is called flat cylindrical perspective (FCP).⁶ Figure 2 shows a diagram representing flat cylindrical perspective and shows the limiting angles involved in determining the field of view. Obviously, it would be desirable to make α large and β small, so as to maximize the viewed surface, but restrictions are imposed on the values of these parameters by the limited range of values of the index of refraction that can be obtained in commercially available glasses. The width of the annular FCP image corresponds to the size of the acceptance angle α , and each concentric ring in the image plane is the locus of points recorded at a fixed angle to the optical axis. Note that since the central portion of the lens is not used to form the image, this region of the lens could be completely removed or used for special purposes.

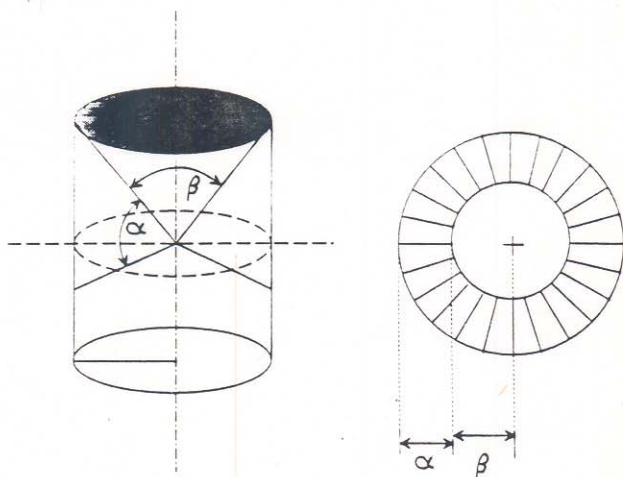


Figure 2. The PAL lens forms an image using flat cylindrical perspective.

Figure 3 shows some rays traced through the PAL and the location of the virtual image formed by the lens. Since the annular image is formed within the PAL itself, it must be transferred to an image capturing device using a collector lens. The most outstanding attributes of the overall system are that there are no moving parts and that the depth of field extends from the surface of the PAL to infinity. A typical PAL has a field of view which extends from about -20 degrees off-axis to about 25 degrees off-axis. As a consequence of the large viewing angle, however, more light is required to capture an image. This is illustrated in Figure 4 which shows that there is a one stop decrease in f-stop when the average intensity recorded from an illuminated screen using a digitizing camera equipped with a 55 mm micro Nikon collector lens is compared with the intensity recorded for the same collector lens used in combination with a PAL. In both cases, the screen was positioned at equal distances from the lens systems.

In various tests and experiments performed so far, the PAL has been used for panoramic imaging and visual inspection,⁷ as a profilometer,^{8,9} and in conjunction with speckle^{10,11} and

holographic^{12,13} measurement techniques. The following sections provide examples and additional details of inspections and measurements made through PAL systems using laser scanning techniques, speckle photography, and holographic interferometry. Computer algorithms for detecting anomalies, digitally correlating images, and linearizing the annular images obtained from the PAL are also discussed.

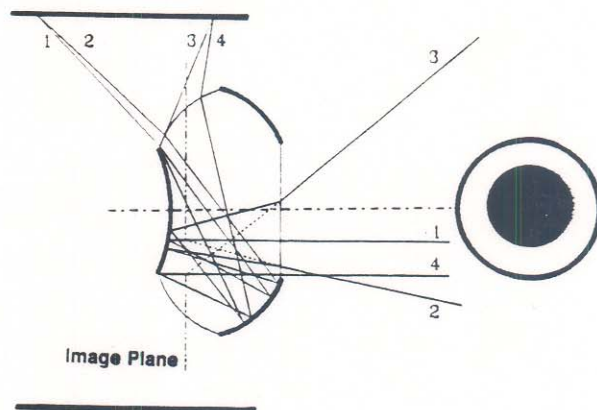


Figure 3. A ray diagram for the PAL.

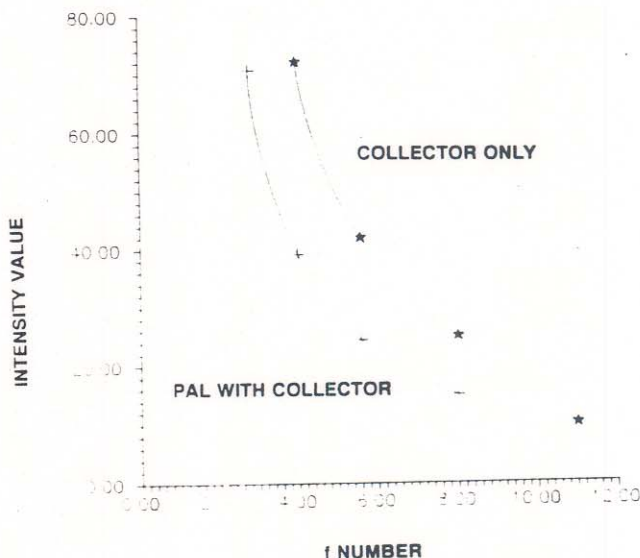


Figure 4. Average intensity values recorded from an illuminated screen with a collector lens alone, and the same collector lens used in combination with a PAL.

Visual Inspection

Figure 5 shows the image obtained when a PAL is positioned along the axis of a cylindrical pipe, the interior surface of which is covered with a test pattern. Even though details are recognizable, direct visual interpretation of the PAL image is

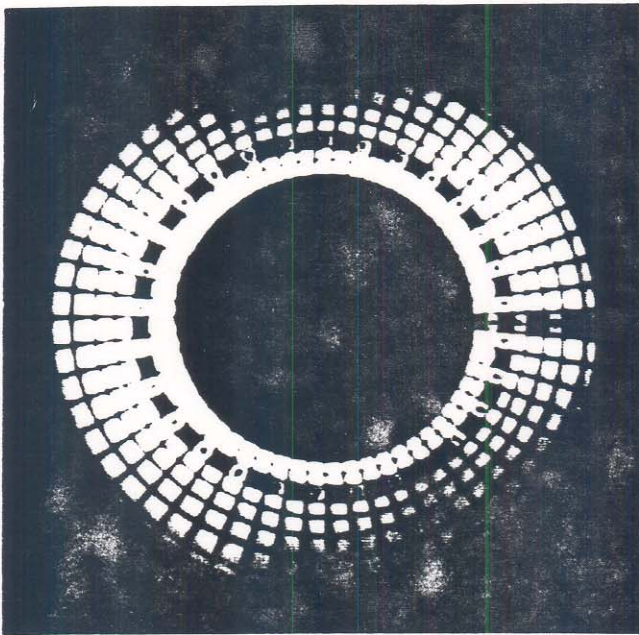


Figure 5. The image obtained when a PAL is positioned along the axis of a cylindrical pipe, the interior surface of which is covered with a test pattern.

often difficult for the unskilled observer. With this in mind, an algorithm was developed to allow the annular images to be linearized for viewing and measuring purposes.⁹ This was accomplished by 'rolling' the annular image along its outer circumference and moving all the pixels between the contact point and the center of the image to a vertical line in the final rectangular image. Figure 6 shows the result of applying the algorithm to the first quadrant of the image shown in Figure 5.

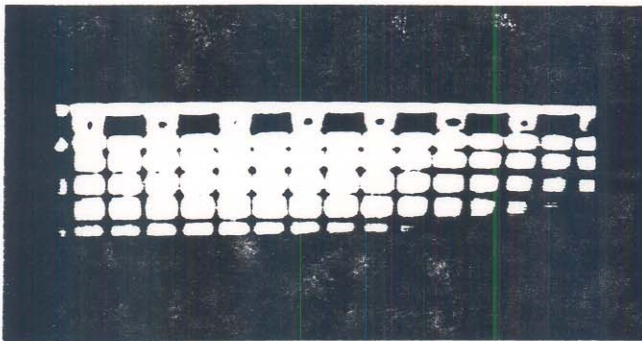


Figure 6. Linearized version of the first quadrant of the image shown in Figure 5.

Such visual inspections are important in many stress analysis applications, especially in cases where chemical deposits cause corrosion, or where combinations of thermal and mechanical stresses cause wear or produce cracks. These conditions are typically encountered in nuclear power plants and in rocket engines where many components, designed to function at high temperatures and pressures, must be periodically inspected to avoid catastrophic failures. Figure 7, for example, is a photograph of an RL10 engine. This engine will be used to

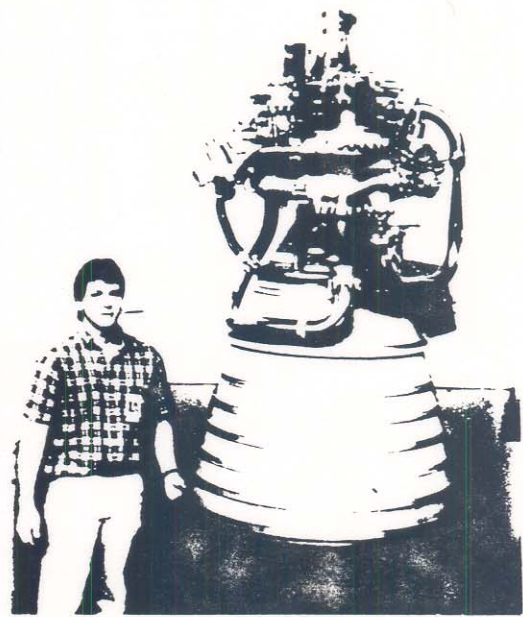


Figure 7. Photograph of an RL10 rocket engine.

launch a number of heavy payloads during the 1990s. Figure 8 shows the panoramic image taken through a PAL system for visual inspection inside the nozzle throat of the engine using a 46 mm diameter PAL.

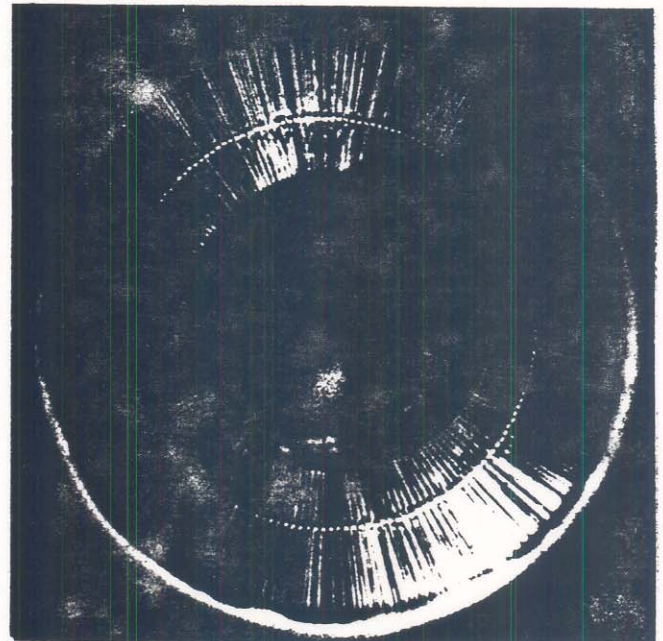


Figure 8. A PAL photograph taken inside the nozzle of an RL10. Photograph provided courtesy of Optechnology, Inc., Huntsville, Alabama.

Probes which incorporate relatively small diameter PALs are currently under development. As shown in Figure 9, a 6.3 mm diameter PAL can be attached to the distal end of a cystoscope. This approach is being developed for use in medical applications to visually inspect human organs.



Figure 9. A 6.3 mm diameter PAL probe.

In addition to cavity inspection, PAL systems are being targeted for use in other interesting engineering applications. Figure 10, for example, illustrates the design for a panoramic imaging system called SEASIS. The imaging system will be contained in an endmass to be deployed from the second stage of a Delta II launch vehicle via a 40 km-long tether.⁷ The panoramic images recorded during the mission will be incorporated with data gathered from a three-axis accelerometer to study tether dynamics. This information will be valuable, since tethered systems will be used in many space-based applications including the construction and use of relatively large tethered platforms. Figure 11, for example, shows a configuration which utilizes space shuttle external tanks in a raft format to form a structure in space. In this example, tethers are used as structural elements in an evolving space station and for links (power, data transfer, etc.) between different platforms designed for various science and applications purposes. Some of the platforms would take advantage of the facilities of the station for maintenance and repair while being isolated from contamination and mechanical disturbances. Others could be used to facilitate storage of liquid propellants and dangerous fluids, or to provide a variable/controlled gravity environment for materials processing or to study long-term effects on humans. In the future, PAL systems may be used to establish accurate frames of reference for such space based construction and could be incorporated into robotic probes to make routine inspections and diagnostic stress analysis measurements.

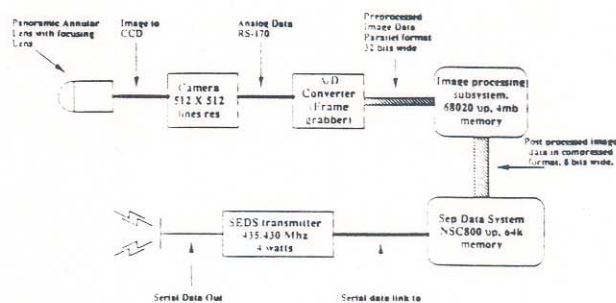


Figure 10. Schematic diagram of SEASIS.

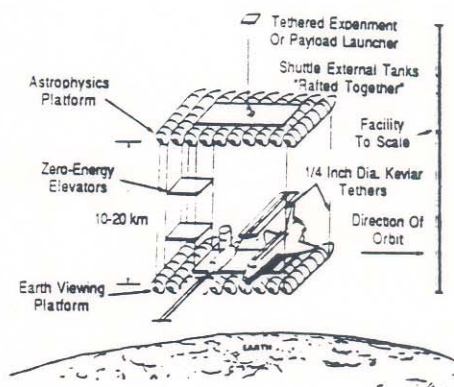


Figure 11. A space platform showing various tether applications.

Profiling

Radial metrology combines an optical measurement technique with the PAL to study the inner surfaces of the cavities found, for example, inside pipes, tubes, and boreholes. The approach can be used for profiling measurements which are important in many practical applications. For example, the infiltration and inflow of ground water into sewer lines and maintenance of collection systems present major problems to a civil engineer. These problems have led to the development of pipeline television systems which are used to inspect sewer lines, as part of new construction acceptance programs, or to troubleshoot a collection system for leaking joints, root intrusion, and protruding taps. Radial metrology enhances visual inspection and will allow a variety of measurements to be performed including the location and size of hairline cracks, the position of offset joints, and the detection of lost aggregate in concrete pipe. The approach may also be important in industrial manufacturing to identify parts outside of set tolerances, and to pinpoint defective or missing components.

Figure 12 illustrates one of the optical configurations evaluated for radial metrology.^{8,9} In this example, a device called a radial profilometer is shown inserted into a cylindrical cavity. A diverging laser beam (shown launched from a fiber optic labeled {1}) is directed through a projection lens {2}. The beam passes through a panoramic annular lens {3} and is

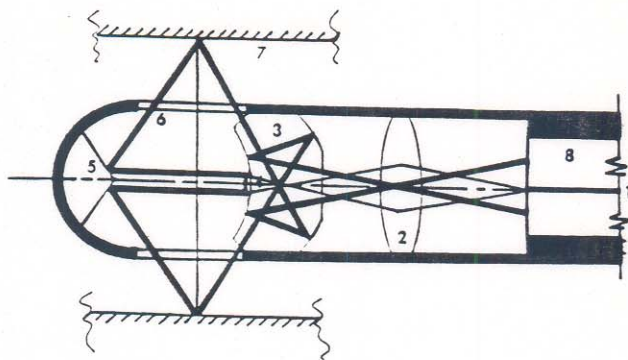


Figure 12. One possible configuration for a radial profilometer.

collimated and shaped by an appropriately masked collimating lens {4} to produce a thin ring. The ring reflects off a conical mirror {5} and passes through a transparent window {6} onto the test surface {7}. The image of the illuminated surface is captured through the transparent window {6} by the panoramic annular lens {3} and is imaged by the projection lens {2} onto a coherent optical fiber bundle {8}. The bundle transmits the image from the device to a computer system where changes in the image can be recorded and analyzed using digital acquisition and processing techniques.

Figure 13 illustrates how a profilometer can be used to visually detect inclusions located on the inner wall of a pipe. In this case, the laser scan which was originally circular traces out shapes in the image plane which are "similar" to those of the inclusions. As demonstrated by Figure 14, computer algorithms can be applied so that quadrants of the image may be linearized

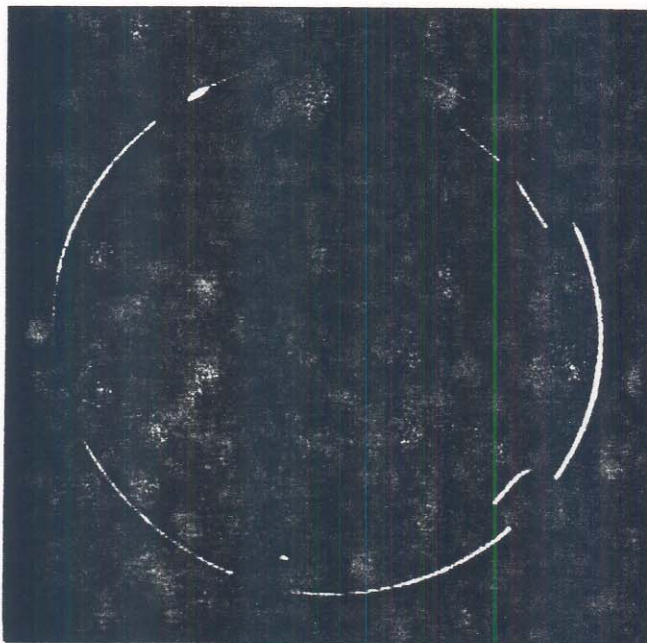


Figure 13. Laser scan over inclusions located on the walls of a cylindrical pipe.

for viewing and measurement purposes. The lower portion of each trace represents a constant radial distance from the optical axis of the profilometer to the wall of the pipe. The shape and dimensions of the inclusions can be easily observed and measured with respect to this baseline. An entire cavity can be profiled simply by moving the profilometer through the cavity; moreover, the measurement system can be designed so that information is extracted based on a linear calibration curve.^{8,9}

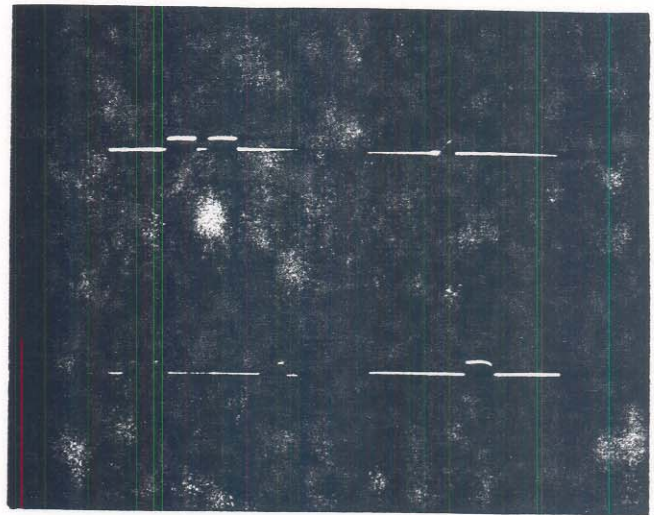


Figure 14. Linearized images for each quadrant of the image contained in Figure 13.

Speckle Metrology

Since the profilometer uses a line scan for profiling, it is necessary to move it through the cavity to obtain measurements over the original field of view. Unfortunately, such a procedure limits functional and real-time capabilities. An alternative method for profiling is to digitally record and numerically correlate artificial speckle patterns projected onto the walls of the cavity. In this case, the profilometer remains stationary during the measurement and data is taken over the full-field.

Digital correlation is a method of pattern recognition in which a small subset of an initial image is located in a second (deformed or displaced) image. A standard equation used to determine the correlation coefficient, ρ , for a window centered over location (m,n) in the displaced image is

$$\rho(m,n) = \frac{\sum_x \sum_y [f(x,y) - \langle f \rangle][w(x-m,y-n) - \langle w \rangle]}{\{\sum_x \sum_y [f(x,y) - \langle f \rangle]^2 \sum_x \sum_y [w(x-m,y-n) - \langle w \rangle]^2\}^{1/2}} \quad (1)$$

where $f(x,y)$ are the intensity values of the second image for those locations under the window values $w(x,y)$ as the window is moved over a suitably chosen search range (x,y) ; $\langle f \rangle$ is the

average intensity value of the region located under the window and $\langle w \rangle$ is the average intensity value of the window. The maximum correlation value indicates the best match of the chosen subset from the initial image as located in the second image.

Since the speckle pattern moves as the shape of the cavity changes, the variation in cavity shape can be measured by applying correlation techniques to the speckle patterns obtained before and after the cavity shape is modified. The apparent speckle movement can be computed by numerically correlating small subsets (windows) extracted from each pattern. These shifts can be used to measure surface deflections or to contour the cavity with respect to a reference shape.

Figure 15 is a schematic of an optical configuration using two opposing collinear PALs which has been evaluated for profiling. A collimated beam of structured light representing a random speckle pattern is introduced into the system at the left and the first PAL projects the speckle pattern onto the walls of the pipe. The second PAL picks up the scattered light and transmits it through a transfer lens to a digitizing camera. The digitizing camera transmits an image similar to the one shown in Figure 16 to a computer where changes in the image can be recorded and analyzed using digital acquisition and processing techniques. Even though sensitivity varies radially with distance from the center of the lens, calibration procedures for speckle projection have established that families of calibration curves can be expressed in closed form.¹⁰ Feasibility tests have been conducted using this technique to measure deformations inside a cylindrical pipe of constant cross section. In this case, deformation was uniform along the longitudinal axis of the pipe.¹⁴ The more general case, in which the geometry of the cavity and the deformation vary as a function of cavity depth, will be addressed in a subsequent paper.

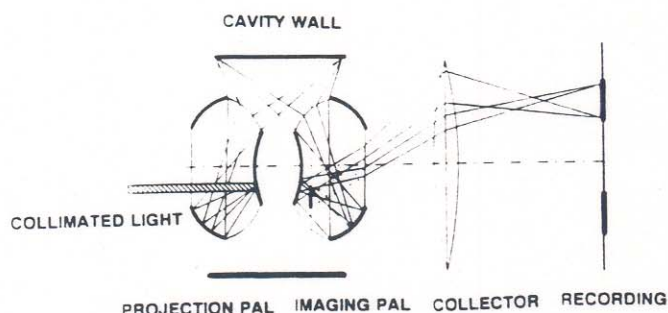


Figure 15. Schematic diagram of a measurement device which relies on two opposing collinear PALs.

Holographic Interferometry

Holo-interferometric fringe patterns may also be recorded within a cavity using the configuration shown in Figure 15. One panoramic annular lens is used to illuminate the cavity wall with coherent light, and the resulting intensity distribution is holographically recorded through the second panoramic

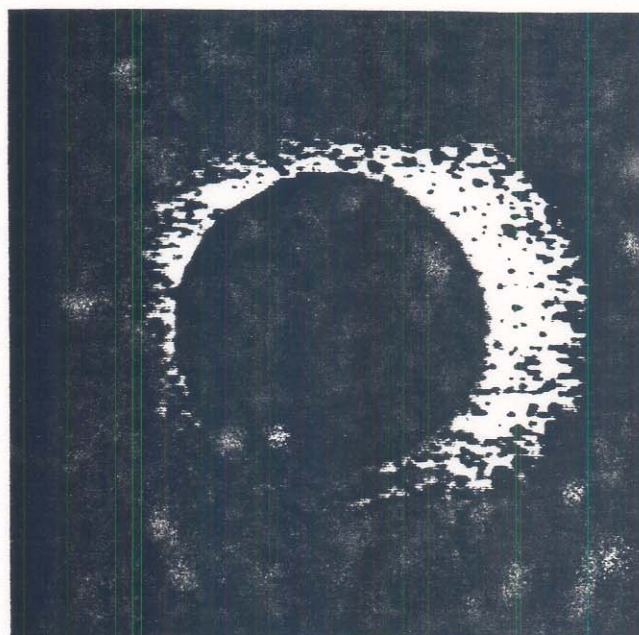


Figure 16. An artificial speckle pattern projected onto the walls of a cavity may be used for profiling.

annular lens. Interference fringes can be obtained in real time by comparing holograms recorded before and after the cavity shape is modified.

The holographic fringes produced when two reconstructed hologram images corresponding to an undeformed and deformed surface are superimposed can be analyzed using

$$n\lambda = \mathbf{g} \cdot \mathbf{d} \quad (2)$$

where n is the fringe order number, λ is the wavelength of the coherent light used to record and reconstruct the hologram and \mathbf{d} is the displacement vector of the surface point under consideration. The sensitivity vector \mathbf{g} is defined by $(\mathbf{e}_2 - \mathbf{e}_1)$ where \mathbf{e}_1 and \mathbf{e}_2 are unit vectors in the direction of illumination and in the direction of observation, respectively.

The observed displacement fringes are due to the change in optical path length which occurs between recordings. These path length changes give rise to a distribution of phase differences between the reconstructed wavefronts which results in areas of constructive or destructive interference and are seen as light and dark fringes. As discussed above, the component of displacement measured at each point depends upon the location of the source and on the point of observation; the displacement vector is projected along the sensitivity vector which coincides with the angle bisector of \mathbf{e}_1 and \mathbf{e}_2 .

When recorded through a PAL, the fringe pattern is first analyzed in the image plane. Then, the values obtained for the corresponding displacement must be mapped to object space by taking into account the separation between the PALs, the radial distance between the test surface and the optical axis of the system, the design parameters of the PALs, and the optical transformations used to illuminate the cavity wall and create the

PAL image. Figure 17, for example, shows a holographic pattern recorded on the wall of a cylindrical pipe as the pipe is translated perpendicular to its longitudinal axis.¹³ A quadrant of the pattern is linearized and compared to theory in Figure 18. A detailed study of this mapping and the corresponding theoretical analysis for holographic fringe patterns recorded through PAL systems will appear in a subsequent paper.

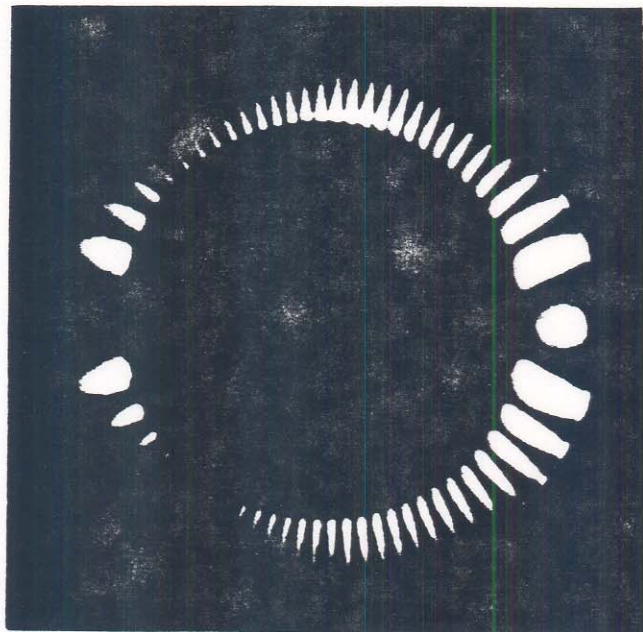


Figure 17. Holographic pattern recorded on the interior wall of a cylindrical pipe for translation normal to the longitudinal axis.

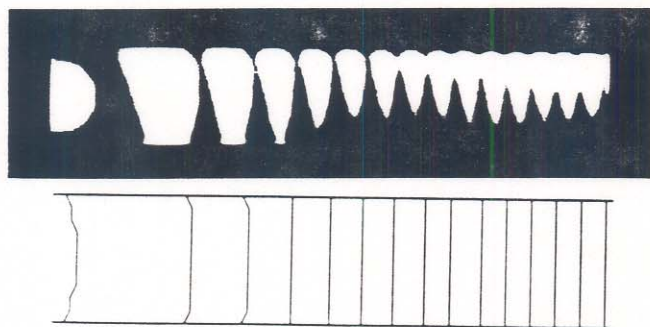


Figure 18. A comparison of the linearized image for the first quadrant of the image shown in Figure 17 with theory.

Conclusions

This paper has described a new panoramic annular lens that produces a flat annular image of the entire 360 degree surround of the optical axis of the lens. Since imaging systems which incorporate the PAL have no moving parts and have an infinite depth of field, cavities can be inspected and measured precisely. The FCP mapping creates an annular image which may be linearized for improved human viewing.

In addition to visual inspection, cavities have been profiled using an approach called radial metrology. Numerous examples of radial metrology have been discussed including amplitude-based measurements conducted by projecting structured patterns onto the cavity walls and phase-based measurements performed using holographic interferometry.

Future publications will discuss the advantages and disadvantages of various configurations proposed for radial metrology and will establish guidelines for further development including automated analysis.

Acknowledgements

The authors wish to acknowledge support provided by the Physics Department at Marquette University, Milwaukee, Wisconsin, the College of Engineering at the University of Alabama in Huntsville, and the Applied Biophysics Laboratory at the Technical University in Budapest. Research in radial metrology has been supported by Optechnology, Inc., Huntsville, Alabama, and NASA's Marshall Space Flight Center under contract numbers NAG-686 and NAG-159.

References

1. Chad, F., French Pat. 1:5.374, 1878.
2. Hill, R., Brit. Pat. 225.398, 1924; Schultz, H., COD 620.538, 1935; Merle, A., DRP 672.393, 1939; Buchelle, D.R., US Pat. 2.638.033, 1950; Majoros, S., Hung. Pat. 143.538, 1954; Brachvogel, H., PRD Pat. 1.135.677, 1960; Bargavist, N., US Pat. 3.984.178, 1976; Wolf, R., Gebrauchsmuster BRD 7.819.433, 1978; Merke, W., Richter, R., von Rohr, M., *Das Photographische Objektiv*, Edward Brothers Inc., Ann Arbor 1948; Oharek, F., "Annular projection lens for 360° nonprogrammed visual display," in the *Report of SORL* Space Optics Research Lab, Chelmsford, Massachusetts 1982.
3. Rees 20 Subminiature CCTV Camera System, Rees Instruments Ltd., Old Woking, England.
4. Downhole TV Camera TT 300, Terratest, Lausanne, Switzerland.
5. Greguss, P., U.S. Patent No. 4,566,763, 1984.
6. Greguss, P., "The tube peeper: a new concept in endoscopy," *Optics and Laser Technology*, 17: 41-45 (1985).
7. Bankston, C.D., Gilbert, J.A., Greguss, P., "Panoramic viewing of a tethered system using SEASIS," *Proc. of the Fourth International Congress on Tethers in Space*, Florence, Italy, October 1-5, 1990.
8. Gilbert, J.A., Greguss, P., Lehner, D.L., Lindner, J.L., "Radial profilometry," *Proc. of the Joint BSSM/SEM International Conference on Advanced Strain Measurement Techniques*, London, England, August 24-27, 1987, Whittles Publishing, pp. 97-107.
9. Greguss, P., Gilbert, J.A., Matthys, D.R., Lehner, D.L., "Developments in radial metrology," *Proc. of SPIE International Symposium on Optical Engineering and Industrial Sensing for Advanced Manufacturing Technologies*, Vol. 954, Dearborn, Michigan, June 25-30, 1988, pp. 392-398.

10. Matthys, D.R., Greguss, P., Gilbert, J.A., Lehner, D.L., Kransteuber, A.S., "Radial metrology with a panoramic annular lens," Proc. of SPIE's 33rd. Annual International Symposium on Optical & Optoelectronic Applied Science & Engineering, San Diego, California, August 6-11, 1989.
11. Gilbert, J.A., Greguss, P., Matthys, D.R., Lehner, D.L., "Recent developments in radial metrology: a computer-based optical method for profiling cavities," Proc. of Optika '88, Third Int. Symp. on Modern Optics, Volume II, Budapest, Hungary, September 13-16, 1988, pp. 413-418.
12. Greguss, P., "Panoramic holocamera for tube and borehole inspection," Proc. of the Int. Seminar on Laser and Optoelectronic Technology in Industry - A State of the Art Review, Xiamen, P.R.C., June 25-27, 1986.
13. Gilbert, J.A., Greguss, P., Kransteuber, A.S., "Holo-interferometric patterns recorded through a panoramic annular lens," Proc. of SPIE's International UNESCO Seminar on 3-D Holography, Volume 1238, entitled 3-D Holography '89, Kiev, USSR, September 5-8, 1989.
14. Matthys, D.R., Gilbert, J.A., Greguss, P., "Radial metrology," submitted for publication to Optical Engineering (April, 1990).